Scattering Parameters Measurement of a Nonreciprocal Coupling Structure

P. Kwan and C. Vittoria, *Fellow, IEEE*

***Abstract*—A novel ferrite image guide was designed and tested from 26.5 to 40 GHz. The nonreciprocal structure consisted of two dielectric image guides separated by a ferrite slab. M-type hexagonal ferrite was used with its C-axis oriented parallel and perpendicular to the direction of propagation. Electromagnetic scattering S -parameters of the device were measured for a nonuniform external biasing magnetic field applied parallel to the C-axis of the ferrite slab. Nonreciprocal effects were observed for all cases considered above. Our results implied applications for ferrite devices operating at millimeter wavelength frequencies, such as: isolators, filters, modulators, switches, phase shifter etc.**

I. Introduction

A MAJOR problem in microwave communication is the congestion of microwave links near or at X -Band. It is only natural that the communication frequency band be extended to millimeter wavelength frequencies. Therefore, there's a great need for millimeter wave components, especially nonreciprocal ferrite components.

Dielectric image guides have been proposed for various millimeter wave integrated circuits including nonreciprocal devices [1]–[5]. As in past developments, ferrites are incorporated in dielectric image guides for this purpose. In particular there have been attempts to calculate the coupling parameters between guides in a structure with an uniform external magnetic field applied along the propagation direction, Fig. 1. Mazur and Mrozowski formulated the problem with the coupling mode method [3], [4]. Sillars and Davis applied the effective dielectric constants method to calculate the coupling coefficient of the same structure [5]. It is well known that the advantage of having the external magnetic field applied along the propagation direction and in the plane of a ferrite slab is that it requires a small field to saturate the ferrite [6]. In their analysis [3]–[4], for this magnetic field direction, $(\vec{H})$, E^y and E^x -modes of propagation in the coupling region was assumed only, the processional motion of the magnetization admixes the E^y and E^x modes of propagation beyond the coupling region. In order to prevent admixing of modes the magnetic field, $\vec{H}$, needs to be applied normal to the ground plane. However, for this field direction, a large external H is required in order to overcome the demagnetizing field in the ferrite.

In this paper we report on the measurement of the scattering S -matrix elements of a four ports microwave device designed by us (Fig. 2). The reference direction is the propagation direction hereafter. We chose the magnetization direction or the C-axis to be along three directions relative to the propagation direction: parallel and perpendicular to it. The C-axis of the ferrite is also defined as the easy axis of magnetization in the ferrite slab ($BaFe_{12-2x}CO_xTi_xO_{19}$). For the C-axis perpendicular to the propagation direction, there are two orthogonal directions of the C-axis or $\vec{H}$-field relative to the propagation direction. $\vec{H}$ was applied only parallel to the C-axis. In Case I, $\vec{H}$ is parallel to the ground plane but transverse to the direction of propagation, and in Case II, $\vec{H}$ is normal to the ground plane. For Case III, the C-axis or $\vec{H}$ field was oriented along the direction of propagation. The external biasing magnetic field $(\vec{H})$ was applied parallel to the C-axis of the ferrite slab.

For the three field directions, we anticipate nonreciprocal behavior in the scattering parameters, since the external biasing field was nonuniform (Fig. 3) as measured along the propagation direction. For a nonuniform static field distribution the precessional amplitude of the magnetization varied along the direction of propagation. Therefore, the coupling between ferrite and electromagnetic wave depended from point to point

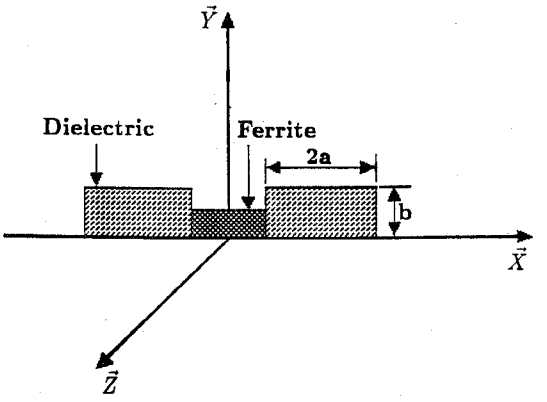

Fig. 1. Cross section of the nonreciprocal structure ($a = 0.95$ mm, $b = 1.7$ mm).

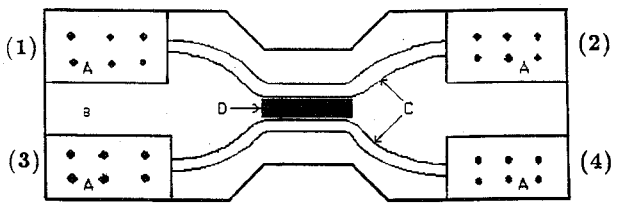

Fig. 2. Top view of the device with out the top metallic plate. (a) Waveguide port (launcher). (b) Ground plane. (c) Dielectric image guide. (d) Ferrite.

Manuscript received December 11, 1992; revised July 31, 1992.

The authors are with the Department of Electrical and Computer Engineering, Northeastern University, Boston, MA 02115.

IEEE Log Number 9206304.

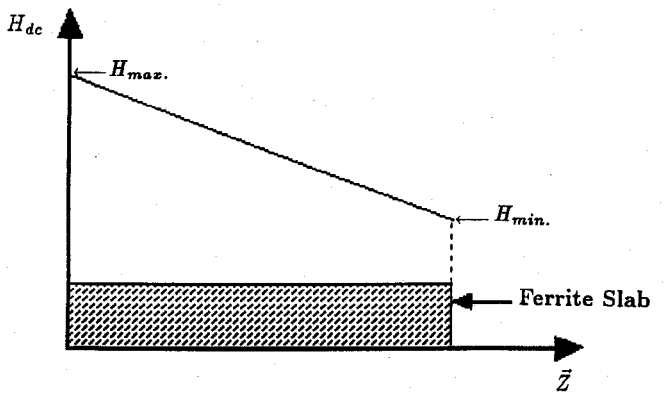

Fig. 3. DC magnetic field distribution along the ferrite slab.

on the ferrite. Since the $\vec{H}$-field variation with distance was uni-directional, the coupling was non-reciprocal with respect to the wave propagation direction. Thus, this implied that the reciprocity property of the coupled structure was not conserved.

We have fabricated a simple device in which two dielectric image guides were coupled via a ferrite slab—Fig. 2. The advantage of this design was that it was possible to observe nonreciprocal effects between any two ports; coupling ports as well as feed through ports. Nonreciprocal effects between the forward transmission and forward coupling (1 and 2, and 1 and 4) were observed, if the external dc magnetic field ($\vec{H}$) was nonuniformily distributed within the ferrite slab.

This paper is organized in the following format. In Section II we have considered the major factors in the design of our device. In Section III we reviewed the experimental procedure of how the electromagnetic scattering parameters were measured. The experimental data is reported in Section IV. Lastly, in Section V we have discussed our results in terms of future alternatives in the design of millimeter wave devices.

II. Device Configuration

The device configuration of Fig. 2. was chosen due to its simplicity of fabrication and analysis. The device was designed to operate at frequencies above 26.5 GHz. The wave guide launcher (Fig. 4) was designed to minimize reflections at the device input. TE_{10} (rectangular wave guide mode) mode of propagation was converted to E_{11}^{y} (image guide mode) mode of propagation. The horn shape was flared at both ends of the launcher for impedance matching purposes, Fig. 4.

Power transmission loss was one of the major factors that one must consider in millimeter wave circuit design. For dielectric image line, there are three types of losses for which one had to be aware of: dielectric, conduction and radiation loss. As Xia *et al.* [1] pointed out, dielectric loss scale nearly linearly with frequency. In order to minimize dielectric loss, a dielectric material with low loss tangent was chosen for the device. Hence, teflon was used ($\epsilon = 2.25(1 - j1 \times 10^{-4})$) with a rectangular cross section of $a = 0.95$ mm and $b = 1.7$ mm. The corresponding cutoff frequency of the dielectric image line was 22.5 GHz.

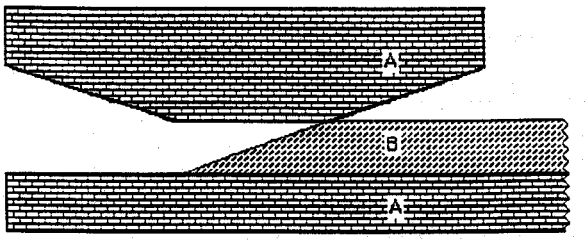

Fig. 4. Wave guide launcher. (a) Conductor. (b) Dielectric.

In general, nonreciprocal devices made use of ferrimagnetic materials to couple the electromagnetic energy to the precessional motion of the ferrite. We chose M-type hexagonal ferrite ($BaFe_{12-2x}CO_xTi_xO_{19}$) with self biasing field for ferrimagnetic resonance. This type of ferrite could provide ferromagnetic resonance without any external biasing field. In order to achieve nonreciprocal effects, only a small nonuniform magnetic field was required.

The dimensions and the characteristics of the ferrite slabs for different cases were tabulated in Table I. Since the dielectric constant (ϵ_r) was relatively high, the coupling between the two dielectric image guides would be reduced due to the large difference in dielectric constants between the ferrite slab and the teflon guides [7]. Equivalently, the characteristic impedance between the ferrite and dielectric medium is mismatched. However, the coupling can be improved by placing a dielectric slab with similar dielectric constant as teflon below and/or above the ferrite slab.

Finally, dielectric image guides may gave rise to radiation loss [8]. To overcome this problem, various methods have been proposed: 1) Itoh introduced the trapped image line [8]. 2) Absorbers placed around the bended regions of the image line [7]. We have placed a metallic plate above the guiding structure in order to reduce the radiation loss. The function of the top plate was to redirect some of the radiated energy back on to the image line [7]. A reduction of approximately 5 dB in the transmission loss has been realized with the top metallic plate in place.

III. Experimental Measurements

The microwave measurements of the scattering matrix elements (S_{ij}) consisted of the following: 1) System Calibration, and 2) Measurements of the S-parameters. The experimental set-up is shown in Fig. 5. In order to improve the accuracy of our measurements (amplitude and phase) calibration of the equipment was essential. Throughout our measurements, the TRL (Through-Reflect-Line) calibration technique was adapted [9]. With the TRL calibration one could eliminate effects due to bending of cables, losses and/or phase shifts in connector junctions. To perform the TRL procedure, the frequency range was conveniently chosen. In order to simulate reflection from a short and open circuits at precise distances from the source, we used a flat waveguide termination and quarter wavelength waveguide flange. However, for simulation of an open circuit load an internal calibration data base located in the HP8510B was used. As the external biasing field

TABLE I

		CASE I	CASE II	CASE III
Dimension (cm)	Length	2.45	2.79	2.05
	Width	0.33	0.30	0.30
	Thickness	0.16	0.163	0.165
Demagnet. Factor	$N_x/4\pi$	0.306	0.345	0.346
	$N_y/4\pi$	0.689	0.652	0.652
	$N_z/4\pi$	0.005	0.003	0.002
	$4\pi M_s$ - (Oe.)	3000	3000	3000
	H_A - (Oe.)	11600.0	11600.0	11600.0
	ε_r	13.0	13.0	13.0
	$H_{max.}$ - (Oe.)	500.0	2500.0	500.0
	$H_{min.}$ - (Oe.)	325.0	2000.0	325.0

increased, we measured the magnitude and changes in phase of the microwave signal.

Let's now discuss the measurements themselves. By definition, S_{11}, reflection coefficient at port 1, was measured when ports 2, 3 and 4 were terminated with match loads. S_{12}, transmission from port 2 to port 1, was measured at port 1 with ports 3 and 4 terminated with match loads. S_{21}, transmission from port 1 to port 2, was measured at port 2 with ports 3 and 4 terminated with match loads. S_{13}, S_{31}, S_{14} and S_{41} were measured as in the same procedure as S_{12} and S_{21}. The return signal from matched loads was approximately 0.25 dB which implied the error in our amplitude measurements was in the order of 0.25 dB. The phase measurement was accurate to ± 5 degrees. The frequency and field measurements were accurate to within 1%.

IV. Experimental Results

Experimental measurements were performed in the frequency range between 26.5 and 40.0 GHz. When the external biasing field was fixed in a given direction, we observed effects due to FMR in the scattering S-parameters. This technique was very helpful in terms of analyzing the nonreciprocal behavior of the device that we built. Nonreciprocal behavior was defined as follows [10]; if S_{ij} was different from S_{ji} with the direction of external magnetic field fixed, then the device behaved nonreciprocally.

Case I

In Case I, the C-axis of the ferrite slab was transverse to the direction of propagation, but parallel to the ground plane. Also, the external magnetic field was applied along the C-axis. We defined magnetic resonance field (H) as that field at which the most changes was observed in $|S_{ij}|$ at a given frequency. Since the range of frequencies was between 26.5 to 40.0 GHz, H was varied between 0 and 1 KOe. We report here results

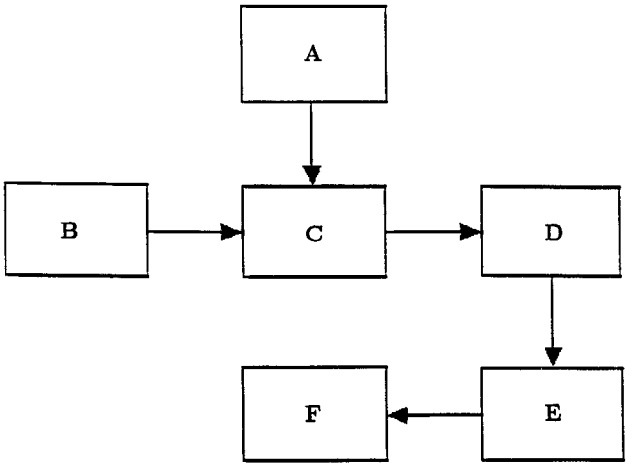

Fig. 5. Experimental Set-Up. (a) Gauss meter. (b) Power supply. (c) Electro-magnet. (d) Device. (e) HP8510B (vector network analyzer). (f) HP9000 (personal computer).

for $H_{\max} = 500$ Oe and $H_{\min} = 325$ Oe ($H_{\max.}$ and $H_{\min}$ are defined in Fig. 3), since the results for other field values were qualitatively and quantitatively similar.

Since there are four ports on the device, there were sixteen scattering coefficients to be measured, S_{ij} where $i, j = 1, 2, 3, 4$. However, there was some redundancy in the measurements. For examples, $S_{11} = S_{22} = S_{33} = S_{44}, S_{31} = S_{42}, S_{41} = S_{32}$, etc. due to the symmetry of the device. The redundancy reduced the complexity of the scattering matrix to the following form:

$$[S] = \begin{pmatrix} S_{11} & S_{12} & S_{13} & S_{14} \\ S_{21} & S_{11} & S_{14} & S_{13} \\ S_{31} & S_{41} & S_{11} & S_{34} \\ S_{41} & S_{31} & S_{43} & S_{11} \end{pmatrix}. \tag{1}$$

This means that only 9 measurements were sufficient to characterize the scattering matrix $[S]$. The matrix $[S]$ was further sub-divided into four sub-matrices. The diagonal sub-matrices were related to transmission properties in the two guides, whereas the off-diagonal sub-matrices corresponded to the coupling between the two image guides. The primary transmission line was the one connecting ports 1 and 2, and between ports 3 and 4, but they were equivalent to each other. Hence, the matrix elements were referred to port 1 mostly. Nonreciprocal behavior was our primary concern here. We now report on the measurements of the forward transmission (ports 1 and 2) and the forward coupling (ports 1 and 4) of the relevant matrix elements of $[S]$. This is justified on the basis that the coupling between ports 1 and 3 was insignificant in comparison to the coupling between ports 1 and 2, and 1 and 4. Also, we observed very little changes in the magnitude of S_{11} as the external field increased from zero up to 1 KOe. This implied that there was a good impedance match at port 1 when ferrimagnetic resonance was excited.

With the direction of H fixed in the $\vec{x}$ direction (Fig. 1) nonreciprocal effects were observed, since the magnitude of S_{21} was different from S_{12} by more than 40 dB at f_o (FMR), Fig. 6(a). This indicated strong nonreciprocal behavior

occurring at FMR. For this case, the FMR condition was given as [6]

$$\left(\frac{\omega}{\gamma}\right)^2 = (H - N_x M_s + H_A) \cdot (H - N_x M_s + N_y M_s + H_A) \quad (2)$$

where $4\pi M_s$ is the saturation magnetization, ω the FMR radial frequency ($\omega = 2\pi f_o$), γ the gyromagnetic ration, H_A the uniaxial anisotropic field and N_x, N_y are the demagnetizing factors along the $\vec{x}$ and $\vec{y}$ directions (Fig. 1), respectively. The FMR frequency was calculated to be 34.1 GHz compared to 35.0 GHz as measured in S_{21}. The FMR frequency was computed assuming a maximum value of H from Fig. 3 or simply $H_{\max}$. At $H_{\max}$ one can assume that the magnetization equals the saturated value. In (2) single domain and full saturation is assumed in calculating the FMR frequency. We have assumed γ to be 2.8 GHz/KOe (see Table I for the values of the other parameters). The demagnetizing factors were determined by the following set of equations:

$$N_x \simeq 8\left(\frac{t}{W}\right)\frac{L}{\sqrt{L^2+W^2}},$$
$$N_y \simeq 8\left(\frac{t}{L}\right)\frac{W}{\sqrt{L^2+W^2}},$$

and

$$N_z \simeq (4\pi - N_x - N_y)$$

where t, W and L are the thickness, width and length of the ferrite slab respectively.

There was strong coupling between ports 1 and 4. The amount of coupling was a function of the separation between the two image lines, operating frequencies etc.. The changes in magnitude due to FMR were quite significant. There was a frequency shift in f_o in the presence of an external biasing $\vec{H}$-field. The difference in magnitude between S_{14} and S_{41} was greater than 30 dB, Fig. 6(b). For this field configuration, we observed very strong nonreciprocal behavior due to FMR in the forward transmission ports as well as in the forward coupling ports. The FMR frequency for S_{41} was different from S_{21}, the shift in f_o was due to phase matching as electromagnetic energy coupled through the ferrite material. This was also an indication of circulation behavior occurring in the device.

Case II

For this case, the C-axis of the ferrite slab was oriented normal to the ground plane. Again, the external biasing field was applied parallel to the C-axis. The external $\vec{H}$ field was varied between 0 and 3 KOe. Here, we report the scattering parameters for $H_{\max.} = 2.5$ KOe. and $H_{\min} = 2.0$ KOe., since the results for other H-field values were qualitatively and quantitatively similar. In addition, there existed a stray magnetic field normal to the C-axis equal to 600 Oe. The reflection coefficient and the coupling between ports 1 and 3 had a very similar behavior as in the previous case.

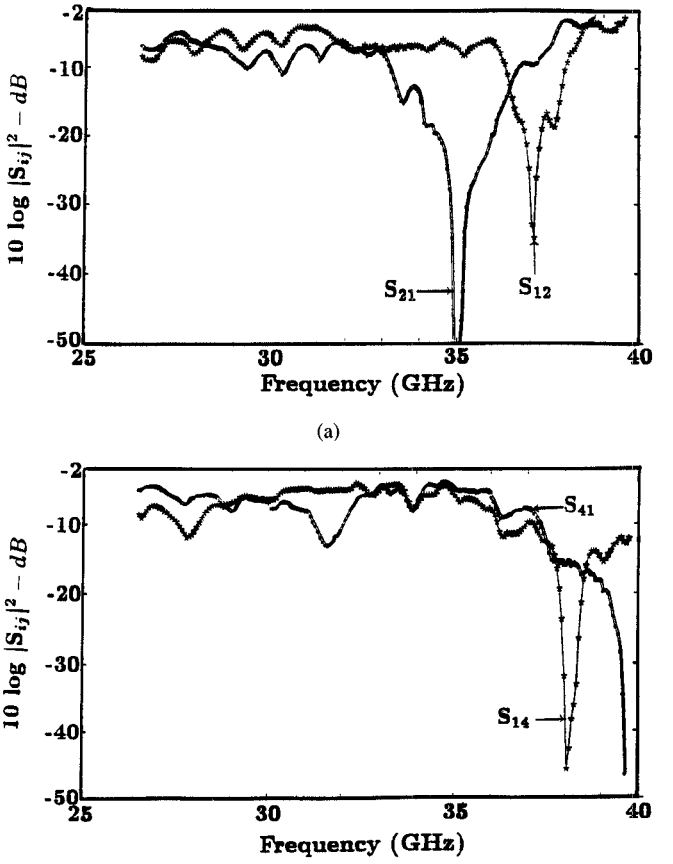

Fig. 6. (a) Forward and reverse transmission for Case I. (b) Forward and reverse coupling for Case I.

In the presence of the external magnetic field, the scatter matrix $[S]$ would take on the following form:

$$[S] = \begin{pmatrix} S_{11} & S_{12} & S_{31} & S_{14} \\ S_{21} & S_{11} & S_{41} & S_{31} \\ S_{31} & S_{14} & S_{11} & S_{12} \\ S_{41} & S_{31} & S_{21} & S_{11} \end{pmatrix}. \quad (3)$$

There are 6 independent scattering parameters in (3). This implied 6 independent measurements are needed in order to characterize the four ports device.

At FMR, the attenuation in the reverse transmission (S_{12}) was approximately 46 dB, but the forward transmission was about 7.5 dB, Fig. 6(a). The amount of attenuation in the reverse coupling (S_{14}) ports was approximately 38 dB, while the forward transmission (S_{41}) was approximately 12 dB at FMR, Fig. 7(b). For $\vec{H}$ applied normal to the ferrite slab, the FMR condition was given as [6]

$$\left(\frac{\omega}{\gamma}\right)^2 = (H - N_y M_s + H_A) \cdot (H + N_x M_s - N_y M_s + H_A) \quad (4)$$

In this field configuration, FMR occurred at higher frequency for the forward transmission (S_{21}) and for the forward coupling (S_{41}). It was clear that nonreciprocal behavior was observed. Also, a higher external biasing H-field was required to excite FMR with $\vec{H}$ normal to the ground plane. The

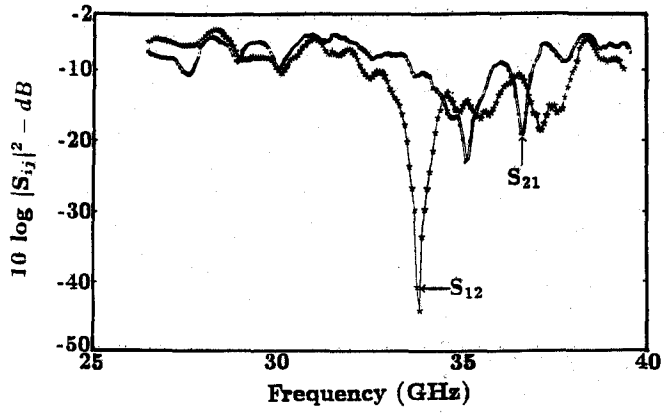

(a)

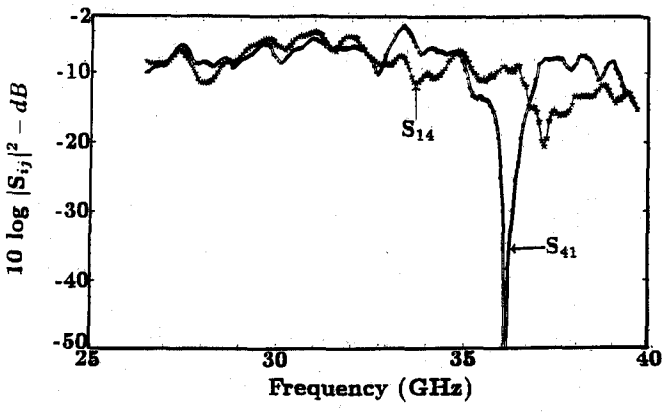

(b)

Fig. 7. (a) Forward and reverse transmission for Case II. (b) Forward and reverse coupling for Case II.

comparison between (4) and the measured FMR frequency is shown in Table II. The calculated value for f_o was 35.4 GHz and the FMR frequency from measurement was 35.2 GHz. Thus, there is a general agreement between the two.

Case III

In this case, the C-axis of the ferrite slab was placed along the propagation direction with the external magnetic field applied parallel to it. We reported here the electromagnetic scattering S-parameters for the magnetic field distributions of 325 to 500 Oe along the propagation direction.

For this field direction the coupling between ferrite material and microwave field is maximum, since the magnetization is perpendicular to the strongest component of the RF magnetic field. As such, non-reciprocal effects are enhanced. Since the non-reciprocal effects are more pronounced for this case, we expect $[S]$ to be less symmetrical than the other two cases. The form of the scattering matrix for this case takes the following form:

$$[S] = \begin{pmatrix} S_{11} & S_{12} & S_{13} & S_{14} \\ S_{21} & S_{11} & S_{14} & S_{24} \\ S_{31} & S_{41} & S_{11} & S_{12} \\ S_{41} & S_{42} & S_{21} & S_{11} \end{pmatrix}. \tag{5}$$

In order to characterize the four ports device fully, now 12 independent measurements are needed.

TABLE II

	CASE I	CASE II	CASE III
f_o - Theo. (GHz)	34.10	35.40	37.70
f_o - Exp. (GHz)	35.00	35.20	36.40
$\|S_{21}\|$ - dB	> 50.00	23.00	19.00
$\|S_{12}\|$ - dB	34.00	44.00	49.00
$\|S_{41}\|$ - dB	46.00	> 50.00	--
$\|S_{14}\|$ - dB	45.00	20.00	37.00

In the reverse transmission (S_{12}), we noticed two different electromagnetic resonances occurring, Fig. 8(a). The narrow frequency band width corresponds to magnetostatic wave excitation in the ferrite slab, [11]. For the forward transmission (S_{21}), the amount of energy being attenuated was not as dramatic as in the previous case. In this field configuration, the FMR condition was given as [6]

$$\left(\frac{\omega}{\gamma}\right)^2 \simeq (H + N_x M_s + H_A) \cdot (H + N_y M_s + H_A) \tag{6}$$

The signal was strongly attenuated in the reverse coupling (S_{14}) at FMR frequency, Fig. 8(b). For the forward coupling (S_{41}), ferrimagnetic resonance seems to occur above 40 GHz. Nevertheless; both signals had strong attenuation in the frequency range of 36 and 40 GHz. The calculated f_o and the measured f_o was found to be in very good agreement.

In summary, strong nonreciprocal effects were observed in Case I, II and III. The amount of attenuation at FMR for the transmission ports (1 and 2) and the coupling ports (1 and 4) is shown in Table II. The calculated and the measured FMR frequency were very close to each other as indicated in Table II. The small amount of error was due to the fringe fields present near the edges.

V. Discussions and Conclusions

Experimental results on a novel four ports device are reported here for three different field configurations. The coupling structure of dielectric image lines comprising of M-type hexagonal ferrite has been fabricated in a planar arrangements operating at millimeter wave frequencies. As expected, nonreciprocal behavior was observed for all $\vec{H}$ field orientations in which $\vec{H}$ was applied along the C-axis of the ferrite. The largest changes in S_{ij} were observed at the upper frequency range for which FMR could be observed. This may be due to the fact that at higher frequencies (or shorter wavelength), the electromagnetic fields were more confined to the image lines. There were strong non-reciprocal behavior observed for all cases. The forward attenuation (S_{21}) was as high as 50 dB at f_o, but the reverse attenuation (S_{12}) was insignificant in comparison to the forward attenuation or vice versa. Thus, the coupling energy is confined to the guided

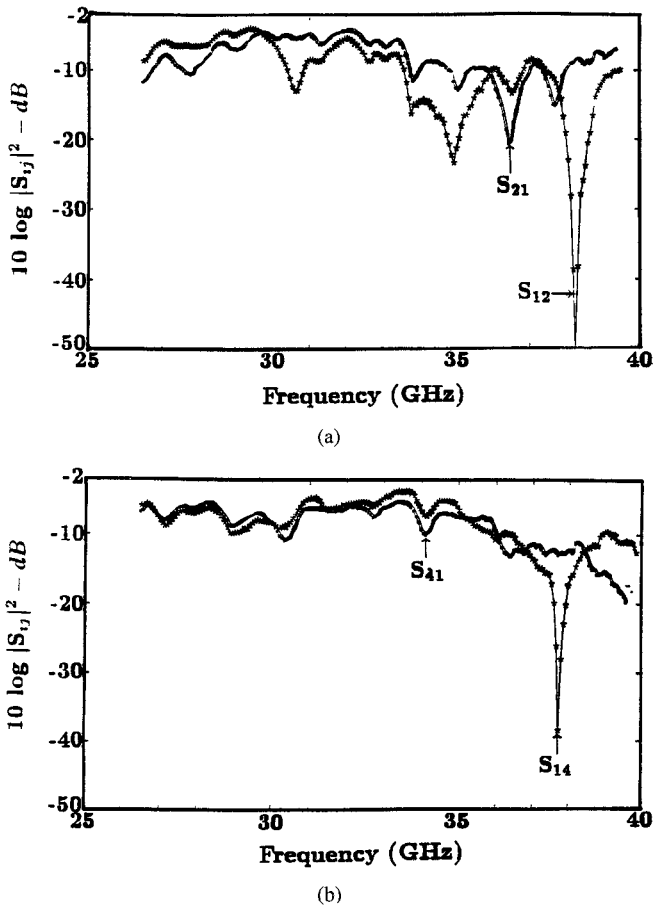

Fig. 8. (a) Forward and reverse transmission for Case III. (b) Forward and reverse coupling for Case III.

structure. The calculated FMR condition compared reasonably well with the resonance behavior of the scattering parameters. This implied that the single domain and saturable medium assumptions are reasonable. We also observed very strong nonreciprocal effects in the forward coupling ports (ports 1 and 4) at the same time, the return loss was not affected by FMR. This was also true for the forward coupling ports. For the field configuration normal to the ground plane (Case II), the E^y mode of propagation was conserved or maintained throughout the frequency range investigated.

In the case where $\vec{H}$ was perpendicular to the ground plane (Case II), significant higher H-field was required for FMR. Nevertheless, it was only necessary to provide a rather small field to observe nonreciprocal effects at high frequencies (26.5–40 GHz). The results presented here could provide a method for nonreciprocal millimeter wave application deploying in planar geometries, such as novel circulator and frequency tuning devices.

ACKNOWLEDGMENT

The authors wish to thank ONR for supporting this project. In addition, we wish to express our appreciation to Dr. H. How for his valuable discussions and Dr. J. Proske of Stackpole Inc. for providing the ferrite materials.

REFERENCES

[1] J. Xia, P. P. Toulios, and C. Vittoria, "Propagation properties of ferromagnetics insular guide," *IEEE Trans. Microwave Theory Tech.*, vol. 37, no. 10, pp. 1547–1554, Oct. 1989.

[2] I. Awai and T. Itoh, "Computed-mode theory analysis of distributed nonreciprocal structures," *IEEE Trans. Microwave Theory Tech* . vol. MTT-29, pp. 1077–1086, Oct. 1981.

[3] J. Mazur and M. Mrozowski, "Nonreciprocal operation of structures comprising a section of coupled ferrite lines with longitudinal magnetization," *IEEE Trans. Microwave Theory Tech.*, vol. 37, no. 6, June 1989.

[4] J. Mazur and M. Mrozowski, "On the mode coupling in longitudinally magnetized waveguiding structures," *IEEE Trans. Microwave Theory Tech.*, vol. 37, pp. 159–165, Jan. 1989.

[5] D. B. Sillars and L. E. Davis, "Analysis of nonreciprocal coupled image lines," *IEEE Trans. Microwave Theory Tech.*, vol. MTT-35, no. 7, pp. 629–635, July 1987.

[6] B. Lax and K. J. Button, *Microwave Ferrite and Ferrimagnetics*. New York: McGraw-Hill, 1962.

[7] D. Kother and I. Wolff, "Image guide couplers with isotropic and anisotropic coupling elements," *Int. J. Infrared and Millimeter Waves*, vol. 9, no. 4, pp. 351–360, Oct. 1988.

[8] W. B. Zhou and T. Itoh, "Analysis of trapped image guides using effective dielectric constant and surface impedances," *IEEE Trans. Microwave Theory Tech.*, vol. MTT-30, no. 12, pp. 2163–2166, Dec. 1982.

[9] R. Pantoja, M. Howes, J. Richardson, and R. Pollard, "Improve calibration and measurement of the scattering parameters of microwave integrate circuits," *IEEE Trans. Microwave Theory Tech.*, vol. MTT-37, no. 37, p. 1675, Nov. 1989.

[10] P. McIsaac, "Bidirectionality in gyrotropic waveguides," *IEEE Trans. Microwave Theory Tech.*, pp. 223–226, Apr. 1976.

[11] R. W. Damon and J. R. Eshbach, "Magnetostatic Modes of a ferromagnetic slab," *J. Phys. Chem. Solids*, vol. 19, p. 308, 1961.

Philip P. Kwan, photograph and biography not available at the time of publication.

C. Vittoria (S'62–M'63–M'80–SM'83–F'90), photograph and biography not available at the time of publication.